Atmos. Chem. Phys. Discuss., 8, 7339–7371, 2008
www.atmos-chem-phys-discuss.net/8/7339/2008/

Atmospheric Chemistry and Physics Discussions

Interpreting the variability of CO_2 columns over North America using a chemistry transport model: application to SCIAMACHY data

P. I. Palmer[1], M. P. Barkley[1], and P. S. Monks[2]

[1]School of GeoSciences, University of Edinburgh, UK
[2]Department of Chemistry, University of Leicester, UK

Received: 18 February 2008 – Accepted: 25 March 2008 – Published: 16 April 2008

Correspondence to: P. I. Palmer (pip@ed.ac.uk)

Published by Copernicus Publications on behalf of the European Geosciences Union.

Abstract

We use the GEOS-Chem chemistry transport model to interpret variability of CO_2 columns and associated column-averaged volume mixing ratios (CVMRs) observed by the SCIAMACHY satellite instrument during the 2003 North American growing season, accounting for the instrument averaging kernel. Model and observed columns, largely determined by surface topography, averaged on a $2^\circ \times 2.5^\circ$ grid, are in excellent agreement (model bias=3%, r>0.9), as expected. Model and observed CVMRs, determined by scaling column CO_2 by surface pressure data, are on average within 3% but are only weakly correlated, reflecting a large positive model bias (10–15 ppmv) at 50–70° N during midsummer at the peak of biospheric uptake. GEOS-Chem generally reproduces the magnitude and seasonal cycle of observed CO_2 surface VMRs across North America. During midsummer we find that model CVMRs and surface VMRs converge, reflecting the instrument vertical sensitivity and the strong influence of the land biosphere on lower tropospheric CO_2 columns. We use model tagged tracers to show that local fluxes largely determine CVMR variability over North America, with the largest individual CVMR contributions (1.1%) from the land biosphere. Fuel sources are relatively constant while biomass burning make a significant contribution only during midsummer. We also show that non-local sources contribute significantly to total CVMRs over North America, with the boreal Asian land biosphere contributing close to 1% in midsummer at high latitudes. We used the monthly-mean Jacobian matrix for North America to illustrate that: 1) North American CVMRs represent a superposition of many weak flux signatures, but differences in flux distributions should permit independent flux estimation; and 2) the atmospheric e-folding lifetimes for many of these flux signatures are 3–4 months, beyond which time they are too well-mixed to interpret.

ACPD

8, 7339–7371, 2008

1 Introduction

The importance of the natural carbon cycle in understanding climate is well established (IPCC, 2007). A better quantitative understanding of natural sources and sinks of carbon dioxide (CO_2), in particular, is crucial if CO_2 mitigation and sequestration activities relying on these natural fluxes are to work effectively. Estimation of sources and sinks of CO_2 using inverted atmospheric transport models to interpret atmospheric concentration data has been generally effective but has had varied success in the tropics where there is relatively little data (Gurney et al., 2002). Previous inversion studies have used surface concentration data (Bousquet et al., 1999), representative of spatial scales of the order of 1000 km by virtue of their location; aircraft concentration data (Palmer et al., 2006; Stephens et al., 2007) representative of spatial scales of the order of 10–100 s km, and generally only available during intensive campaign periods; and concentrations from tall towers (Chen et al., 2007), representative of spatial scales of the order of <1–10 s km.

New CO_2 column data from low-Earth orbit space-borne sensors (e.g., the Scanning Imaging Absorption Spectrometer for Atmospheric Chartography (SCIAMACHY) (Bovensmann et al., 1999), the Orbiting Carbon Observatory (OCO) (Crisp et al., 2004; Miller et al., 2007), and the Greenhouse Observating SATellite (GOSAT) (Hamazaki et al., 2004)), measuring in the near-infrared (NIR), are sensitive to changes in CO_2 in the lower troposphere and therefore provide potentially useful data with which to estimate surface fluxes of CO_2 (Chevallier et al., 2007). One of the main advantages of space-borne sensors is their repeated global coverage, facilitating measurements, for example, over remote tropical ecosystems that are currently poorly characterized by in situ data. SCIAMACHY CO_2 data, in particular, are representative of a 60 km×30 km spatial footprint, comparable with the horizontal resolution of current generation atmospheric transport models; upcoming instruments will have better horizontal resolution. At the time of writing, SCIAMACHY is the only space-borne sensor in orbit that measures CO_2 columns sensitive to the lower troposphere. To date there have been very

ACPD
8, 7339–7371, 2008

few model studies of SCIAMACHY CO_2 column data, which have provided only qualitative comparisons (Buchwitz et al., 2005, 2007; Barkley et al., 2006c). In this paper, we use the GEOS-Chem global 3-D chemistry transport model (CTM) to interpret the variability in CO_2 columns from SCIAMACHY over North America during the 2003 growing season. We focus on North America because of the extensive multi-platform measurement programme which can be used to help evaluate SCIAMACHY via the CTM.

A number of studies have illustrated that the precision and accuracy of measured CO_2 columns is critical to their success in better quantifying the carbon cycle. The temporal and spatial variations in column data are much less than those in surface concentration measurements (Olsen and Randerson, 2004). Inversions of synthetic data have shown that CO_2 columns have to be retrieved with a precision of less than 1% over a 8°×10° grid if they are to improve upon the existing ground-based network used for source/sink estimation (Rayner and O'Brien, 2001). Consequently, uncharacterized systematic biases will compromise this ability (Miller et al., 2007). Use of column CO_2 has the benefit of effectively reducing the potential model bias introduced by inaccurate descriptions of vertical mixing (Olsen and Randerson, 2004). Nonetheless, recent work has highlighted the requirement of using accurate, synoptic-scale atmospheric transport to interpret CO_2 column data in order to minimize errors associated with spatial sampling, particularly over geographical regions with active weather systems (Corbin et al., 2008). The vertically integrated CO_2 column abundance represents the sum of an age-spectrum of airmasses. Young airmasses (defined in this paper as <3 months), still bearing the signatures of surface fluxes, are subject to atmospheric dilution processes that eventually render these signatures indistinguishable from the global background whose variability is determined by atmospheric transport. In this paper we show that variability in space-borne CO_2 columns over one region is determined by both national and international surface flux signatures (local biosphere fluxes that reach 1.1% of the column-averaged volume mixing ratio, CVMR, generally represent the largest signals) that can be used to estimate flux strengths via inverse model calculations. We also emphasize that accounting for the vertical sensitivity of

the satellite instrument can, in some instances, enhance surface flux signatures.

Section 2 briefly describes the SCIAMACHY retrievals of CO_2 used in this work and presents CO_2 distributions over North America. Section 3 describes the GEOS-Chem CTM used for this study and presents a brief model evaluation using surface CO_2 data over North America from the GLOBALVIEW network (GLOBALVIEW-CO_2, 2006). Section 4 critically examines the comparison between model and SCIAMACHY CO_2 columns and CVMRs. In Sect. 5 we use the model to estimate which land-based fluxes determine the continental-scale variability of CVMRs over North America during the growing season, and look in detail at two contrasting sites over North America. In Sect. 6 we discuss how CVMRs data could be used to infer source and sink distributions. We conclude the paper in Sect. 5.

2 SCIAMACHY CO_2 data

SCIAMACHY is a nadir and limb-viewing UV/Vis/NIR solar backscatter instrument aboard the ENVISAT satellite, launched in 2002 (Bovensmann et al., 1999). It measures from 240 to 2380 nm, with a resolution of 0.2–1.4 nm depending on the channel. ENVISAT is in a near-polar sun-synchronous orbit crossing the equator at about 10:00 local solar time in the descending node, achieving full longitudinal global coverage at the equator within six days. SCIAMACHY makes measurements in an alternating nadir and limb sequence. We use the nadir measurements that have a horizontal resolution of $60\times30\,km^2$ (across × along track).

We include here only a short description of the retrieval of SCIAMACHY CO_2 and refer the reader to dedicated retrieval studies (Buchwitz et al., 2000; Barkley et al., 2006a). CO_2 columns are retrieved in the 1561.03–1585.39 nm wavelength window using the Full Spectral Initiation (FSI) (Barkley et al., 2006a) Weighting Function Modified Differential Optical Absorption Spectroscopy (WFM-DOAS) (Buchwitz et al., 2000). The mean fitting uncertainty of these columns is typically 1–4% (0.8–3.2×10^{20} molec cm^{-2} based on a fitted column of 8×10^{21} molec cm^{-2}), which is largely

attributable to poor characterization of the atmospheric state (e.g., aerosols, cirrus clouds) (Barkley et al., 2006a). Cloudy scenes are diagnosed using the SCIAMACHY polarization measurement devices using a cloud algorithm developed by Krijger et al. (2005), as described by Barkley et al. (2006a), and excluded from subsequent analyses. We also exclude back scans, observations with solar zenith angles >75° (Barkley et al., 2006a), and observations over ocean due to very low surface albedo. We use only observations with a retrieval error of <5% and within a range of 340–400 ppmv (to adequately constrain the light path). Previous studies have extensively evaluated FSI CO_2 data against independent measurements over the Northern Hemisphere. Comparisons between SCIAMACHY CO_2 and ground-based Fourier Transform Spectrometers (FTS) and a CTM show a negative bias of 2–4% in the absolute CVMRs magnitudes. Strong correlations between SCIAMACHY CO_2 anomalies and aircraft and ground-based data imply that SCIAMACHY can track lower troposphere variability on at least monthly timescales, and has the potential to monitor changes in CO2 (Barkley et al., 2006b, c, 2007). At this time, several retrieval issues (e.g., aerosol contamination) need to be resolved before the data are characterized sufficiently well for inverse modelling.

Figure 1 shows monthly mean CO_2 columns (molec cm^{-2}) over North America during the 2003 growing season (here defined as April–September) averaged over the GEOS-Chem 2°×2.5° grid (Sect. 3). Observed columns represent the vertical integral of atmospheric CO_2 weighted by the instrument averaging kernel that describes the instrument sensitivity to changes in the vertical profile of CO_2. As we show later in Sect. 3 SCIAMACHY has most sensitivity to CO_2 in the lower troposphere (Barkley et al., 2006c). The average number of individual scenes that fall into a North American 2°×2.5° grid box is between 25 and 50, depending on month; this effectively reduces the random error by approximately an order of magnitude. Outside the growing season spatial coverage at high latitudes is reduced by seasonally varying solar zenith angle and persistent cloud cover. Retrieved columns range from 6 to 8×10^{21} molec cm^{-2} with the largest values during Springtime over the Northeast and the smallest values gener-

ally later in the summer. The spatial distribution of CO_2 columns is determined largely by surface topography, with the Rockies mountain range introducing an apparent longitudinal gradient across North America.

To remove artefacts introduced by surface elevation we normalize retrieved CO_2 columns using the nearest 6-hourly 1.125°×1.125° ECMWF model surface pressure (Barkley et al., 2006c) to derive a CVMR. As we discuss in Sect. 4 there is significantly less agreement between model and observed values of CVMR than column abundances. Figure 2 shows monthly mean SCIAMACHY CO_2 CVMRs from April to September 2003 over North America. Values range from 350 to 390 ppmv with a 15–20 ppmv peak-to-peak seasonal cycle over regions with a strong biospheric signal, consistent with previous studies (Olsen and Randerson, 2004). Other studies of SCIAMACHY CO_2 data have used O_2 columns to normalize retrieved CO_2 columns, to derive a dry air CVMR, (Buchwitz et al., 2007). Using O_2 instead of surface pressure will partially cancel effects of aerosols and clouds on the light path. However, at the time of writing the general efficacy of this approach is not well quantified owing to differences between the radiative transfer and subsequent averaging kernels of the CO_2 and O_2 spectral fitting windows. Future satellite missions (e.g., OCO and GOSAT) also plan to use O_2 to normalize derived CO_2 columns.

3 The GEOS-Chem forward model of CO_2: description and evaluation

We use the GEOS-Chem global 3-D chemistry transport model (v7-03-06) to calculate column concentrations of CO_2 from prescribed surface CO_2 fluxes described in this section. We used the model with a horizontal resolution of 2°×2.5°, with 30 vertical levels (derived from the native 48 levels) ranging from the surface to the mesosphere, 20 of which are below 12 km. The model is driven by GEOS-4 assimilated meteorology data from the Global Modeling and Assimilation Office Global Circulation Model based at NASA Goddard. The 3-D meteorological data is updated every six hours, and the mixing depths and surface fields are updated every three hours. The CO_2 simulation

is based on Suntharalingam et al. (2004) and Palmer et al. (2006); here, we provide a description of modifications to these previous studies.

3.1 CO_2 flux inventories

Table 1 reports the regional monthly mean estimates of CO_2 fluxes from fuel combustion (sum of fossil fuel and biofuel), biomass burning, and the land biosphere used in GEOS-Chem. Gridded fossil fuel emission distributions are representative of 1995 (Suntharalingam et al., 2004) which we have scaled to 2003 values using regional budget estimates for the top 20 emitting countries in 2003 from the Carbon Dioxide Information Analysis Center (Marland et al., 2007), including sources from fossil fuel burning, gas flaring, and cement production. On a global scale the sum of these sources has increased by 14% relative to 1995 values. Biofuel emission estimates, taken from Yevich and Logan (2003), represent climatological values. This source of CO_2 is generally less than 1% of the total fuel source for North America and western Europe but represents up to 18% of the total fuel source for Asia. In many regions, particularly Asia, the distributions of fossil and bio-fuel emissions overlap significantly so we lump these fuel source together (FL). Monthly biomass burning (BB) emission estimates are taken from the second version of the Global Fire Emission Database (GFEDv2) for 2003 (van der Werf et al., 2006). These data are derived from ground-based and satellite observations and should describe well the burning distributions. Monthly mean air-sea fluxes of CO_2 are taken from Takahashi et al. (1999). As we show later the observed variability in SCIAMACHY data is determined largely by continental fluxes so we do not discuss further the role of ocean exchange in this study. We use daily mean land biosphere (BS) fluxes from the CASA model for 2001 (Randerson et al., 1997), in the absence of corresponding fluxes for 2003. Year-to-year variability of CASA monthly mean land biosphere CO_2 fluxes is small (<10%) so our approach should not introduce significant error. We do not explicitly account for the contribution of fuel combustion CO_2 from the oxidation of reduced carbon species (Suntharalingam et al., 2005) as they make only a small contribution to the CO_2 column.

3.2 Model initialization

CO_2 concentrations for January 2002 were initialized from a previously evaluated model run (Palmer et al., 2006), which we integrate forward to January 2003. We include an additional intialization to correction for the model bias introduced by not accounting for the net uptake of CO_2 from the terrestrial biosphere. We make this downward correct by comparing the difference between GLOBALVIEW CO_2 data (GLOBALVIEW-CO_2, 2006) and model concentrations over the Pacific during January 2003. Differences range from 1 to 4 ppmv with a median of 3.5 ppmv, and we subtract this value globally, following Suntharalingam et al. (2004).

From January 2003 the total CO_2 tracer becomes the "background" CO_2 concentration and is only subject to atmospheric transport. At that time, we also introduce additional model tracers, initialized with a uniform value (for numerical reasons and which is subtracted in subsequent analyses), that account for the monthly production and loss of CO_2 originating from specific geographical regions and surface processes. The linear sum of these monthly tagged tracers (and the "background") is equivalent to the total CO_2. Figure 3 shows the tagged geographical regions for these experiments: North America (NA), Europe (EU), Asia (AS), Boreal Asia (BA), and the rest of the World (ROW). We separately account for CO_2 contributions from fossil fuel emissions (FF), biofuel emissions (BF), biomass burning (BB), the land biosphere (BS), the ocean biosphere (OC), and the inert initial conditions from January 2003. As mentioned above, FL describes the sum of FF and BF. We find the ocean flux contribution to atmospheric CO_2 columns is diffuse and is difficult to distinguish from the initial conditions and is consequently lumped with the ROW.

3.3 Evaluation of model North American surface CO_2 concentrations

Figure 4 presents a comparison of model and GLOBALVIEW measurements (GLOBALVIEW-CO_2, 2006) of surface CO_2 concentrations over North America during 2003. Here, we have chosen measurement sites that include reasonable coverage

in 2003 and that have contrasting seasonal cycles. We sample the model at the location of each measurement site and at the time that SCIAMACHY passes over each site, to illustrate the extent to which SCIAMACHY can observe the seasonal cycle over North America. For example, there is no data in early 2003 over Canada because of persistent cloud. In general, the 2°×2.5° model has some skill in reproducing the in situ surface concentration data but there are some notable exceptions where the model overestimates observed concentrations by nearly 10 ppmv during periods of CO_2 uptake (Fraserdale and Harvard Forest) and mistimes the land biosphere uptake by a few weeks (Park Falls). As we show later in Sect. 4 these examples of model error are not necessarily explained only by local North American fluxes but also by other continental fluxes.

3.4 Modelling CO_2 columns and CVMRs from SCIAMACHY

Global 3-D model CO_2 distributions are sampled at the time and location of the SCIAMACHY scenes. We take into account the vertical sensitivity of SCIAMACHY to changes in CO_2 by using the instrument averaging kernel, **A**. The averaging kernel formally describes the sensitivity of retrieved CO_2 columns to changes in CO_2 throughout the column, and is a reflection of atmospheric radiative transfer at NIR wavelengths. Figure 5 shows the mean SCIAMACHY averaging kernel, averaged over solar zenith angles ranging from 0° to 70°, increase in sensitivity throughout the troposphere with only a small fall-off in the last 1 km (Barkley et al., 2006c). As noted above, not taking **A** into account compromises subsequent interpretation of observed columns. Model SCIAMACHY CO_2 columns, Ω, are given by (Rodgers, 2000)

$$\Omega = \Omega_a + \mathbf{a}(\mathbf{H}(\mathbf{x}) - \mathbf{x}_a), \quad (1)$$

where $\mathbf{H}(\mathbf{x})$ is the GEOS-Chem forward model, $\mathbf{x}_a$ is the a priori CO_2 concentration profile taken from climatology and also used in the SCIAMACHY retrievals (Remedios et al., 2006) and Ω_a is the associated column. The column averaging kernel **a** is given

by $\mathbf{t}^T\mathbf{A}$, where $\mathbf{t}$ is the column integration operator that integrates a vertical profile to a column and the superscript T denotes the matrix transpose operation.

The tagged column contributions to the total CO_2 columns, corresponding to geographical regions in Fig. 3 and source types discussed above, are calculated by weighting the model vertical profile by the column averaging kernel: $\Omega_{tag}=\mathbf{a}[\mathbf{H}(\mathbf{x})]_{tag}$.

Model CO_2 CVMRs are determined by scaling each model column by its nearest GEOS-4 surface pressure value, taking into account unit changes. We used $1^\circ\times1.125^\circ$ GEOS-4 surface pressure data to be consistent with a) the horizontal resolution of the ECWMF surface pressure data used in the SCIAMACHY retrieval, and b) the $2^\circ\times2.5^\circ$ GEOS-4 meteorology used in the GEOS-Chem model.

4 Comparison of model and observed CO_2 columns and CVMRs

Figure 1 shows model CO_2 columns (molec cm^{-2}) are generally within 3% of the observed columns, consistent with (Barkley et al., 2006c), and describe more than 80% of the observed variability. As discussed earlier, column distributions are largely determined by changes in surface topography, and consequently a reflection of the surface pressure fields. However, it is clear that model and observed columns show the largest disagreement over the North and East during periods of biospheric uptake (denoted by red data in the Fig. 1 scatterplot). Model bias, used throughout this paper, is defined as:

$$\text{bias} = 100\frac{1}{n}\sum_{i=1}^{n}\frac{\Omega_i^m - \Omega_i^o}{\max(\Omega_i^m, \Omega_i^o)}, \quad (2)$$

where Ω^o is the observed column, Ω^m is the model column, and n is the number of observations.

Figure 2 shows the model and observed CVMRs (ppmv). Observed CVMRs generally show a larger East-West gradient (10–15 ppmv) than the model (5–6 ppmv). Model

ACPD
8, 7339–7371, 2008

CVMRs generally have a narrower dynamic range compared with the observations, largely confined between 360 to 390 ppmv. Differences between model and observed CVMRs during each month is approximately Gaussian centred away from zero (not shown). Unlike SCIAMACHY CO we find no significant correlation between model and data differences and the spectral fitting uncertainty (de Laat et al., 2007) . On average the model is within 3% of the observed CVMRs, but this reflects a large positive bias of low observed CVMRs and small negative bias of high observed columns. The large positive bias is largely due to the model underestimating columns over the eastern US and at higher latitudes (denoted by red data points in Fig. 2 scatterplot), where vegetation is predominant, but will also include an unquantified component from measurement uncertainty. On a continental scale, the model has relatively little skill in reproducing SCIAMACHY CVMRs, capturing only a few percent of the observed variability, which is determined mainly by the dipole in CO_2 column oriented NW-SE, characteristic of the seasonal biospheric uptake (Barkley et al., 2006b, c; Buchwitz et al., 2007). However, as we show in Sect. 4 the model does have skill in reproducing SCIAMACHY data at individual GLOBALVIEW stations.

Figure 6 shows the North American model and SCIAMACHY CO_2 CVMRs and model surface VMRs expressed as a zonal mean. The zonal mean removes much of the valuable spatial structure but 1) highlights the zonal mean bias between the model and SCIAMACHY, and 2) reveals the dramatic 10 ppmv decrease in SCIAMACHY CO_2 CVMR during the mid-summer months at latitudes between 50 to 70° N. The corresponding decrease in model CVMR is only 5 ppmv. We also note that during mid-summer when the biospheric uptake of CO_2 peaks the model CVMR and surface CO_2 concentrations converge, reflecting the increasing influence of land biosphere on the lower tropospheric column. This implies that that measured columns will be most sensitive to surface processes during mid-summer when biospheric uptake is at its peak, which has implications for surface flux estimation. Previous studies of CO_2 column (e.g. Olsen and Randerson, 2004) have not reported this finding, which in our study is due to the averaging kernel peaking at near-surface altitudes (Fig. 5). As we show

later, outside of the peak North American growing period other CO_2 sources and sinks play a comparable role in determining the column distribution.

5 What surface fluxes determine model CO_2 CVMR variability over North America?

5.1 Continental-scale distributions

Figure 7 shows the land-based contributions to CO_2 CVMRs over North America (Fig. 3 and Table 1). Many source and sink terms show large seasonal cycles in their CVMR contributions. Background CO_2 CVMRs (January 2003 initial conditions in our calculations, Sect. 3) are typically greater than 350 ppmv (not shown).

CO_2 columns over North America are determined largely by local sources and sinks, as expected. The North American land biosphere (BS NA) represents the single largest contribution to total CO_2, with a minimum and maximum of −8 ppmv and 3 ppmv, respectively, corresponding to a maximum of 1.1% of the total column. This contribution, here determined by the CASA model (Sect. 3), is a source of CO_2 until late May, after which it becomes a sink peaking in July. During periods of uptake it is characterized by a dipole with uptake over the North and East and a source over the arid southwestern states Barkley et al. (2006b, c). A similar pattern is evident in model and observed total columns and CVMRs (Figs. 1 and 2). Fuel sources from North America (FL NA) are relatively constant in magnitude throughout the year (Table 1), with the largest CVMR contributions over the East coast (up to 0.5 ppmv). The North American biomass burning (BB NA) season starts in Canada in June reaching a peak in August with partial monthly mean columns of 1 ppmv; this contribution, in particular, is likely to be much larger on sub-monthly timescales and finer spatial scales.

We also show that CO_2 columns over North America are significantly influenced by Boreal Asia and mainland Asia and that in some months these column contributions are comparable in magnitude to North American fluxes. Column contributions

ACPD
8, 7339–7371, 2008

from Boreal Asian fuel sources (FL BA) are largest over Alaska and northern Canada, reflecting the latitude of Boreal Asia and subsequent atmospheric transport. Similar spatial distributions are shown for biomass burning and the land-biosphere from Boreal Asia (BS BA), with the contribution from biomass burning peaking in mid-summer. The land-biosphere is most positive during April (1.2 ppmv) and is most negative during July (−5 ppmv). The seasonal cycle of BS BA is similar to that of the North American biosphere (BS NA), which may compromise the ability of column observations to independently estimate fluxes from the North American and Boreal Asian biospheres despite exhibiting different spatial distribution in column space. The largest mainland Asian fuel and biomass burning contributions (FL AS, BB AS) to North American CO_2 occur in March (not shown) and April over the west Coast, consistent with current understanding of the temporal continental outflow from that region (Liu et al., 2003). The biospheric signal from mainland Asia (BS AS) is delayed relative to North America with a negative peak in August. European column contributions from fuel, biomass burning, and the land biosphere (FL EU, BB EU, BS EU) are qualititively similar to Boreal Asia, reflecting similar high latitude atmospheric transport, but they are an order of magnitude smaller.

Many of these sources and sinks will be much higher on sub-monthly temporal scales and on finer spatial scales but our results reiterate previous studies that emphasize the importance of sub-1% precision column measurements if physically meaningful surface flux distributions of CO_2 are to be estimated.

5.2 Temporal distributions at individual sites

Figures 8 and 9 show the CO_2 flux signatures that determine the variability of CO_2 at two measurement sites: the WLEF television tower, 12 km east of Park Falls in Wisconsin and Wendover in Utah. Earlier, in Fig. 4, we showed that GEOS-Chem had some skill in reproducing the seasonal cycle of CO_2 at both these sites, but predicted premature uptake of CO_2 at the Parks Falls site. We chose these two sites for this analysis because they exhibit different seasonal cycles.

As in Fig. 4 we sample the model at the location of the two ground-based sites and at the SCIAMACHY overpass time when data is available. The WLEF site shows a seasonal cycle with a peak-to-peak range of 20 ppmv, which is captured reasonably well by GEOS-Chem. The corresponding model CO_2 columns vary by 3×10^{20} molec cm^{-2}, representing a change of order 4% in the column. SCIAMACHY reproduces the broad-scale seasonal cycle observed at the surface (and the tower data at this site (Barkley et al., 2007)) but because of noise, due to the retrieval and the relatively coarse spatial colocation (Barkley et al., 2007), it is difficult to assess whether SCIAMACHY reproduces the later onset of the uptake observed by surface measurements. We use a 30-point running mean to effectively reduce random noise. The resulting smoothed observed columns, even after accounting for the bias, show a larger drawdown of CO_2 during midsummer. Model and observed CVMRs show greater discrepancy during midsummer months. Figure 8d shows the seasonal contributions of different monthly sources and sinks to model CVMRs >0.5 ppmv at some time during the year. Fuel combustion from North America, Europe and mainland Asia increase throughout the year, as expected, with a mean gradient of 1.5 ppmv/year. The North American biosphere at this site makes a significant contribution to the total CO_2 CVMR, with smaller but significant contributions from Boreal Asia, Europe and mainland Asia. The different continental biosphere signals peak at different times, due to differences in seasonal cycles and atmospheric transport. Biomass burning from Boreal Asia plays only a small role in determining CO_2 CVMRs at this site, peaking in the Spring. Based on this calculation it is difficult to attribute differences between model and observed CO_2 CMVRs to bias in the magnitude or timing of different continental biosphere fluxes. However, as we discuss in the next section these subtle differences may help to spatially disaggregate CO_2 fluxes using formal inverse models.

Figure 9 shows model and observed columns and CVMRs at Wendover, Utah. The seasonal cycle at this site is weaker than at WLEF, with a peak-to-peak range of 10 ppmv. SCIAMACHY (smoothed) columns have a negative bias similar in magnitude to observed columns at the WLEF site. Model and observed CVMRS are gen-

erally much noisier than at WLEF, reflecting rapid variations in relatively small values of GEOS-4 surface pressure (790–840 hPa compared with 960–990 hPa at WLEF). Apparent drawdown of observed and model CO_2 columns and CVMRs at this site is much weaker than at the WLEF site. Figure 9d shows the seasonal contributions of different monthly sources and sinks to model CVMRs >0.5 ppmv at some time during the year. As at WLEF there is a strong fuel signature originating from North America, Europe, and mainland Asia with a similar gradient through the year. From our analysis the weak seasonal cycle is determined by biospheric signals from Boreal and mainland Asia, which is not obvious from interpreting total column data.

6 Implications for surface flux estimation

The ultimate goal of space-borne CO_2 data are to locate and quantify natural sources and sinks of CO_2 so that more detailed studies can assess their durability with changes in climate. Generally, an inverse model is required for that purpose. While such a study is outside the scope of this paper, and will be the subject of forthcoming work, we calculate the monthly mean Jacobian matrix corresponding to our forward model calculations to illustrate the ability of these column data to infer individual sources and sinks of CO_2. In general the Jacobian matrix, describing the sensitivity of total CO_2 columns to changes in surface sources and sinks, attributes differences between forward model (GEOS-Chem) and observed quantities to specific surface sources and sinks.

For illustration only, Fig. 10 shows the monthly mean columns of the Jacobian matrix for North America, based on Fig. 7 and Table 1. These calculations show that the North America and Boreal Asia land biosphere signals are among the strongest signals that can potentially be retrieved independently. While the initial goal of inversions of space-based CO_2 data may be to estimate total fluxes on a continental scale, it is clear that the superposition of different continental flux signatures (some which represent 1% of total CVMRs) complicates the interpretation of such data. However, as we discussed

earlier and show in Fig. 7 the distributions of many of the dominant flux signatures are sufficiently separated in space and time to permit independent estimation of individual fluxes; this needs to be confirmed with inversion calculations. Many of the sources and sink of CO_2 shown here will have much stronger signatures on finer temporal and spatial scales and that should also be considered.

The e-folding lifetime of these individual flux contributions is typically 3 to 4 months, with e-folding lifetimes exceeding 6 months for Asian sources, consistent with Bruhwiler et al. (2005). All sensitivities converge to a background sensitivity (20) beyond which individual source and sink signatures are well mixed. In practice, the inversion will use a Jacobian matrix for a specific surface grid box to avoid aliasing and to capture the sharp temporal gradients in CO_2 during the onset and decline of the growing season.

7 Conclusions

We have used the GEOS-Chem global 3-D CTM, driven by a priori sources and sinks of CO_2, to interpret variability of SCIAMACHY CO_2 columns. We have shown that GEOS-Chem has some skill in reproducing observed distributions of surface VMR at sites over North America. The magnitude and distribution of model CO_2 columns, accounting for the SCIAMACHY averaging kernel, are determined largely by surface pressure and show good agreement with SCIAMACHY (r=0.9) as expected but with a 3% positive bias. Model CO_2 CVMRs show much less agreement, partly driven by a large positive bias in drawdown of CO_2 during the growing season. We show that model CVMRs and surface VMRs converge during peak growing season months, a result amplified by the use of the SCIAMACHY averaging kernels that describe how instrument sensitivity increases as a function of depth in the troposphere. This suggest that SCIAMACHY and upcoming instruments sensing CO_2 at NIR wavelengths will be most sensitive to periods of intense biospheric uptake (Barkley et al., 2007).

We have used a tagged approach to interpret variability of CVMRs in terms of individual source and sink terms. In general, we find local sources provide the largest

contributions to CVMR variability, with the North American land biosphere representing more than 1% during peak growing season. Fuel sources are relatively constant, while biomass burning makes only a significant contribution in mid-burning season. Our calculations show that surface fluxes from Boreal Asia, mainland Asia and Europe also represent significant contributions to CVMR variability over North America, with, for instance, the Boreal Asia land biosphere responsible for almost 1% of the total CVMR in mid-summer. While there are significant overlaps in the CVMR distributions from local and non-local fluxes, there is also sufficient separation of these contributions in time and space that with careful analysis should permit independent flux estimation. Analysis of data from individual sites within the US provided further insight into the superposition flux signatures. At the WLEF GLOBALVIEW site near Park Falls, Wisconsin we showed that the seasonal cycle (peak-to-peak surface VMR of 29 ppmv) was driven by North American biospheric uptake (−4 ppmv peak) but also biospheric uptake signatures from Boreal Asia, Europe and to a lesser extent mainland Asia. In contrast, the site at Wendover Utah, with a smaller peak-to-peak seasonal cycle of 10 ppmv had large contributions from biospheric uptake signatures originating from Boreal Asia and mainland Asia, both peaking in late summer with CVMRs of −2 ppmv.

CO_2 flux estimation relies partly on quantifying the difference between model and observed CO_2 quantities. Prescribed error covariance matrices describe only the random error associated with the model and observations. Uncharacterized systematic error could be mis-attributed to surface source and sinks. Estimating systematic bias with a model is of little value because our current quantitative understanding of the carbon cycle is incomplete. Dedicated calibration-validation efforts are underway for upcoming spaceborne missions. A particular focus, owing to spatial nature of the column data, is the estimation of regional biases (on spatial scales of 100 km), a length scale lying between undetectable effects due to noise and large-scale biases detectable with precise and accurate ground-based FTS. Unfortunately, no such measurements were available during 2003. Recent studies have shown that SCIAMACHY CO_2 columns VMRs during 2004 are within 2% of the ground-based FTS column measurements at Park Falls,

Wisconsin, capturing only the monthly mean variability (Barkley et al., 2007). This suggests that CO_2 CVMR anomalies might be more effective than CO_2 CVMRs as the measurement vector.

Acknowledgements. P. I. Palmer acknowledges NERC grant NE/F000014/1, M. P. Barkley acknowledges NERC grant NE/D001471/1, and P. S. Monks acknowledges NERC CASIX and DARC funding.

References

Barkley, M. P., Frieß, U., and Monks, P. S.: Measuring atmospheric CO_2 from space using the Full Spectral Initiation (FSI) WFM-DOAS, Atmos. Chem. Phys., 6, 3517–3534, 2006a, http://www.atmos-chem-phys.net/6/3517/2006/. 7343, 7344

Barkley, M. P., Monks, P. S., and Engelen, R. J.: Comparison of SCIAMACHY and AIRS CO_2 measurements over North America during the summer and autumn of 2003, Geophys. Res. Lett., 33, L20805, doi:10.1029/2006GL026807, 2006b. 7351

Barkley, M. P., Monks, P. S., Frieß, U., Mittermeier, R. L., Fast, H., Körner, S., and Heimann, M.: Comparisons between SCIAMACHY atmospheric CO_2 retrieved using (FSI) WFM-DOAS to ground based FTIR data and the TM3 chemistry transport model, Atmos. Chem. Phys., 6, 4483–4498, 2006c, http://www.atmos-chem-phys.net/6/4483/2006/. 7342, 7344, 7345, 7348, 7349, 7350, 7366

Barkley, M. P., Monks, P. S., Hewitt, A. J., Machida, T., Desai, A., Vinnichenko, N., Nakazawa, T., Arshinov, M. Y., Fedoseev, N., and Watai, T.: Asssessing the near-surface sensitivity of SCIAMACHY atmospheric CO_2 retrieved using (FSI) WFM-DOAS, Atmos. Chem. Phys., 7, 3597–3619, 2007, http://www.atmos-chem-phys.net/7/3597/2007/. 7353, 7355, 7357

Bousquet, P., Ciais, P., Peylin, P., Ramonet, M., and Monfray, P.: Inverse modeling of annual atmospheric CO_2 sources and sinks: 1. method and control inversion, J. Geophys. Res., 104, 26 161–26 178, 1999. 7341

Bovensmann, H., Burrows, J. P., Buchwitz, M., Frerick, J., Nöel, S., Rozanov, V. V., Chance, K. V., and Goede, A. H. P.: SCIAMACHY - Mission objectives and measurement modes, J. Atmos. Sci., 56, 127–150, 1999. 7341, 7343

Bruhwiler, L. M. P., Michalak, A. M., Peters, W., Baker, D. F., and Tans, P.: An improved Kalman Smoother for atmospheric inversions, Atmos. Chem. Phys., 5, 2691–2702, 2005, http://www.atmos-chem-phys.net/5/2691/2005/. 7355

Buchwitz, M., Rozanov, V. V., and Burrows, J. P.: A near-infrared optimized DOAS method for the fast global retrieval of atmospheric CH_4, CO, CO_2, H_2O, and N_2O total column amounts from SCIAMACHY Envisat-1 nadir radiances, J. Geophys. Res., 105, 15 231–15 246, 2000. 7343

Buchwitz, M., de Beek, R., Burrows, J. P., Bovensmann, H., Warneke, T., Notholt, J., Meirink, J. F., Goede, A. P. H., Bergamaschi, P., Körner, S., Heimann, M., and Schulz, A.: Atmospheric methane and carbon dioxide from SCIAMACHY satellite data: initial comparison with chemistry and transport models, Atmos. Chem. Phys., 5, 941–962, 2005, http://www.atmos-chem-phys.net/5/941/2005/. 7342

Buchwitz, M., Schneising, O., Burrows, J. P., Bovensmann, H., Reuter, M., and Notholt, J.: First direct observation of the atmospheric CO_2 year-to-year increase from space, Atmos. Chem. Phys., 7, 4249–4256, 2007, http://www.atmos-chem-phys.net/7/4249/2007/. 7345, 7350

Chen, J. M., Chen, B., and Tans, P.: Deriving daily carbon fluxes from hourly CO_2 mixing ratios measured on the WLEF tall tower: An upscaling methodology, J. Geophys. Res., 112, G01015, doi:10.1029/2006JG000280, 2007. 7341

Chevallier, F., Breon, F., and Rayner, P. J.: Contribution of the Orbiting Carbon Observatory to the estimation of CO_2 sources and sinks: Theoretical study in a variational data assimilation framework, J. Geophys. Res., 112, D09307, doi:10.1029/2006JD007375, 2007. 7341

Corbin, K. D., Denning, A. S., Lu, L., Wang, J.-W., and Baker, I. T.: Possible representation errors in inversions of satellite CO_2 retrievals, J. Geophys. Res., 113, D02301, doi:10.1029/2007JD008716, 2008. 7342

Crisp, D., Atlas, R. M., Breon, F. M., Brown, L. R., Burrows, J. P., Ciais, P., Connor, B. J., Doney, S. C., Fung, I. Y., Jacob, D. J., Miller, C. E., O'Brien, D., Pawson, S., Randerson, J. T., Rayner, P., Salawitch, R. J., Sander, S. P., Sen, B., Stephens, G. L., Tans, P. P., Toon, G. C., Wennberg, P. O., Wofsy, S. C., Yung, Y. L., Kuang, Z., Chudasama, B., Sprague, G., Weiss, B., Pollock, R., Kenyon, D., and Schroll, S.: The Orbiting Carbon Observatory (OCO) mission, Adv. Space Res., 34, 700–709, 2004. 7341

de Laat, A. T. J., Gloudemans, A. M. S., Aben, I., Krol, M., Meirink, J. F., van der Werf, G. R., and Schrijver, H.: Scanning Imaging Absorption Spectrometer for Atmospheric Chartography carbon monoxide total columns: statistical evaluation and comparison with chemistry transport model results, J. Geophys. Res., 112, D12310, doi:10.1029/2006JD008256, 2007. 7350

GLOBALVIEW-CO_2: GLOBALVIEW-CO_2: Cooperative Atmospheric Data Project – Carbon

Dioxide, CD-ROM, NOAA GMD, Boulder, Colorado (Also available via anonymous FTP to ftp.cmdl.noaa.gov, path: ccg/co2/GLOBALVIEW), 2006. 7343, 7347, 7365

Gurney, K. R., Law, R. M., Denning, A. S., Rayner, P. J., Baker, D., Bousquet, P., Bruhwiler, L., Chen, Y.-H., Ciais, P., Fan, S., Fung, I. Y., Gloor, M., Heimann, M., Higuchi, K., John, J., Maki, T., Maksyutov, S., Masarie, K., Peylin, P., Prather, M., Pak, B. C., Randerson, J., Sarmiento, J., Taguchi, S., Takahashi, T., and Yuen, C.-W.: Towards robust regional estimates of CO_2 sources and sinks using atmospheric transport models, Nature, 415, 626–630, doi:10.1038/415626a, 2002. 7341

Hamazaki, T., Kuze, A., and Kondo, K.: Sensor system for Greenhouse gas Observing SATellite (GOSAT), Proc. SPIE, 5543, doi:10.1117/12.560589, 2004. 7341

IPCC: Climate Change 2007 – The Physical Basis, Contribution of Working Group I to the Fourth Assessment Report of the IPCC, Cambridge University Press, iSBN 978 0521 880099-1, 2007. 7341

Krijger, J. M., Aben, I., and Schrijver, H.: Distinction between clouds and ice/snow covered surfaces in the identification of cloud-free observations using SCIAMACHY PMDs, Atmos. Chem. Phys., 5, 2279–2738, 2005, http://www.atmos-chem-phys.net/5/2279/2005/. 7344

Liu, H. Y., Jacob, D. J., Bey, I., Yantosca, R. M., Duncan, B. N., and Sachse, G. W.: Transport pathways for Asian combustion outflow over the Pacific: Interannual and seasonal variations, J. Geophys. Res., 108(D20), 8786, doi:10.1029/2002JD003102, 2003. 7352

Marland, G., Boden, T. A., and Andres, R. J.: Global, Regional, and National CO_2 Emissions, in: Trends: A Compendium of Data on Global Change, Tech. rep., Carbon Dioxide Information Analysis Center, Oak Ridge National Laboratory, US Department of Energy, Oak Ridge, Tenn., USA, 2007. 7346

Miller, C. E., Crisp, D., DeCola, P. L., Olsen, S. C., Randerson, J. T., Michalak, A. M., Alkhaled, A., Rayner, P., Jacob, D. J., Suntharalingam, P., Jones, D. B. A., Denning, A. S., Nicholls, M. E., Doney, S. C., Pawson, S., Boesch, H., Connor, B. J., Fung, I. Y., O'Brien, D., Salawitch, R. J., Sander, S. P., Sen, B., Tans, P., Toon, G. C., Wennberg, P. O., Wofsy, S. C., Yung, Y. L., and Law, R. M.: Precision requirements for space-based X_{CO_2} data, J. Geophys. Res., 112, D10314, doi:10.1029/2006JD007659, 2007. 7341, 7342

Olsen, S. C. and Randerson, J. T.: Differences between surface and column atmospheric CO_2 and implications for carbon cycle research, J. Geophys. Res., 109, D02301, doi:10.1029/2003JD003968, 2004. 7342, 7345, 7350

Palmer, P. I., Suntharalingam, P., Jones, D. B. A., Jacob, D. J., Streets, D. G., Fu, Q., Vay, S. A.,

and Sachse, G. W.: Using CO_2:CO correlations to improve inverse analyses of carbon fluxes, J. Geophys. Res., 111, D12318, doi:10.1029/2005JD006697, 2006. 7341, 7346, 7347
Randerson, J. T., Thompson, M. V., Conway, T. J., Fung, I. Y., and Field, C. B.: The contribution of terrestrial sources and sinks to trends in the seasonal cycle of atmospheric carbon dioxide, Global Biogeochem. Cycles, 11, 535–560, 1997. 7346
Rayner, P. J. and O'Brien, D. M.: The utility of remotely sensed CO_2 concentration data in surface source inversions, Geophys. Res. Lett., 28, 175–178, 2001. 7342
Remedios, J. H., Parker, R. J., Panchal, M., Leigh, R. J., and Corlett, G.: Signatures of atmospheric and surface climate variables through analyses of infrared spectra (SATSCAN-IR), in: Proceedings of the first EPS/METOP RAO workshop, ESRIN, 2006. 7348
Rodgers, C. D.: Inverse methods for atmospheric sounding, World Scientific, 2000. 7348
Stephens, B. B., Gurney, K. R., Tans, P. P., Sweeney, C., Peters, W., Bruhwiler, L., Ciais, P., Ramonet, M., Bousquet, P., Nakazawa, T., Aoki, S., Machida, T., Inoue, G., Vinnichenko, N., Lloyd, J., Jordan, A., Heimann, M., Shibistova, O., Langenfelds, R. L., Steele, L. P., Francey, R. J., and Denning, A. S.: Weak Northern and Strong Tropical Land Carbon Uptake from Vertical Profiles of Atmospheric CO_2, Science, 316, 1732–1735, 2007. 7341
Suntharalingam, P., Jacob, D. J., Palmer, P. I., Logan, J. A., Yantosca, R. M., Xiao, Y., and Evans, M. J.: Improved quantification of Chinese carbon fluxes using CO_2/CO correlations in Asian outflow, J. Geophys. Res., 109, D18S18, doi:10.1029/2003JD004362, 2004. 7346, 7347
Suntharalingam, P., Randerson, J. T., Krakauer, N., Jacob, D. J., and Logan, J. A.: The influence of reduced carbon emissions and oxidation on the distribution of atmospheric CO_2: implications for inversion analysis, 19, GB4003, doi:10.1029/2005GB002466, 2005. 7346
Takahashi, T., Wanninkhof, R. T., Feely, R. A., Weiss, R. F., Chapman, D. W., Bates, N. R., Olafsson, J., Sabine, C. L., and Sutherland, C. S.: Net sea-air CO_2 flux over the global oceans, in: Proceedings of the 2nd international symposium CO_2 in the oceans: CGER 1037, pp. 9–15, National Institute for Environmental Studies, Tsukuba, Japan, 1999. 7346
van der Werf, G. R., Randerson, J. T., Giglio, L., Collatz, G. J., Kasibhatla, P. S., and Arellano Jr., A. F.: Interannual variability in global biomass burning emissions from 1997–2004, Atmos. Chem. Phys., 6, 3423–3441, 2006, http://www.atmos-chem-phys.net/6/3423/2006/. 7346
Yevich, R. and Logan, J. A.: An assessment of biofuel use and burning of agricultural waste in the developing world, Global Biogeochem. Cycles, 17, 1095, doi:10.1029/2002GB001952, 2003. 7346

Table 1. Monthly mean regional CO_2 fluxes (Tg CO_2/month) for the forward model analysis (Sect. 3 and Fig. 3). BB denotes biomass burning; FL denotes the sum of fossil fuel and biofuel combustion; and BS denotes the land biosphere. ROW includes only land-based sources and sinks; the ocean biosphere is an annual global net sink of −8050 Tg CO_2/yr. Boreal Asia (BA) is defined by 72.5° E–172.5° W, 45° N–88° N; mainland Asia (AS) is defined by 72.5° E–152.5° E, 8° N–45° N; Europe (EU) is defined by 17.5° E–72.5° W, 36° N–88° N; North America (NA) defined by 172.5° E–17.5° E, 24° N–88° N; and the rest of the world (ROW) is the remaining region.

	Jan	Feb	Mar	Apr	May	Jun	Jul	Aug	Sep	Oct	Nov	Dec
BB												
BA	0	0	21	124	486	233	196	80	26	13	1	0
AS	29	37	93	89	15	5	4	5	5	4	3	9
EU	0	0.5	6	21	17	6	14	39	34	30	0.3	0.2
NA	2	1	3	6	7	44	36	95	22	14	9	1
ROW	895	463	360	262	891	774	801	853	669	427	360	668
FL												
BA	53	47	53	51	53	51	53	53	51	53	51	53
AS	808	730	808	730	808	730	808	808	730	808	730	808
EU	570	514	570	551	570	551	570	570	551	570	551	570
NA	563	508	563	545	563	545	563	563	545	563	545	563
ROW	475	429	475	460	475	460	475	475	460	475	460	475
BS												
BA	374	401	563	657	64	−1469	−1818	−952	459	770	542	408
AS	288	484	763	797	243	−363	−916	−1141	−456	−12	127	180
EU	534	455	333	−98	−1068	−1491	−1284	−307	651	892	772	630
NA	703	709	729	496	−248	−1692	−1981	−1167	33	834	838	747
ROW	−101	−322	−350	119	−139	−1385	−1431	−578	952	1363	1099	771

ACPD
8, 7339–7371, 2008

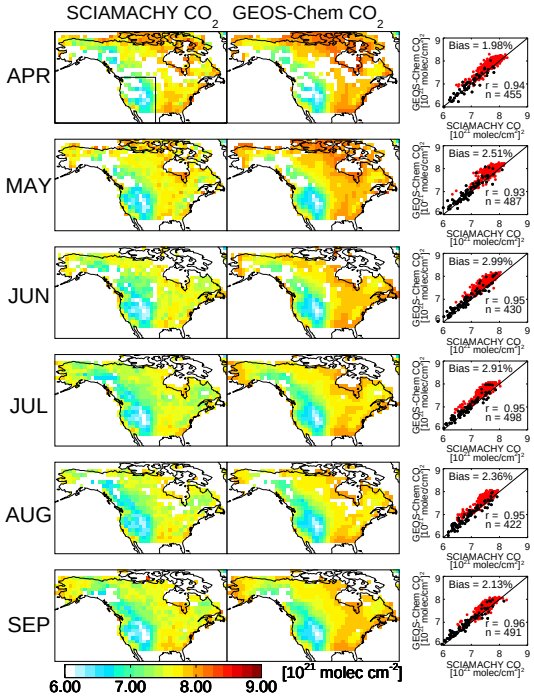

Fig. 1. Monthly mean SCIAMACHY (left) and GEOS-Chem (middle) CO_2 columns (10^{21} molec cm^{-2}) over North America during April to September 2003 averaged over the GEOS-Chem 2°×2.5° grid. The model is sampled at the time and location of the observed scenes, and using the SCIAMACHY averaging kernel as outlined in the main text. The RHS panels show scatterplots of the monthly mean data, with the number of data points n, correlation coefficient r, and the model bias inset. Red data denote columns over the region defined by latitudes >50° N and longitudes >100° W (as shown in top LHS panel). We exclude 1) cloudy scenes, identified by instrument polarization devices, 2) scenes with solar zenith angles >75°, 3) scenes with a retrieval errors of ≥5%, and 4) scenes that correspond to CVMRs outside of the range 340–400 ppmv.

ACPD
8, 7339–7371, 2008

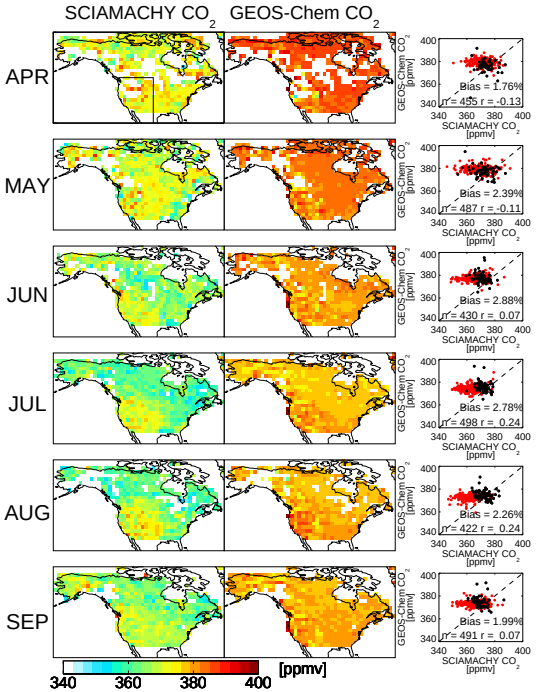

Fig. 2. Monthly mean SCIAMACHY and GEOS-Chem CO_2 CVMRs (ppmv) over North America during April to September 2003 averaged over the GEOS-Chem 2°×2.5° grid. The model and data descriptions are as Fig. 1. The nearest ECMWF (1.125°×1.125°) and GEOS-4 (1°×1.125°) surface pressure data are used to convert from observed and model columns to CVMRs, respectively.

ACPD
8, 7339–7371, 2008

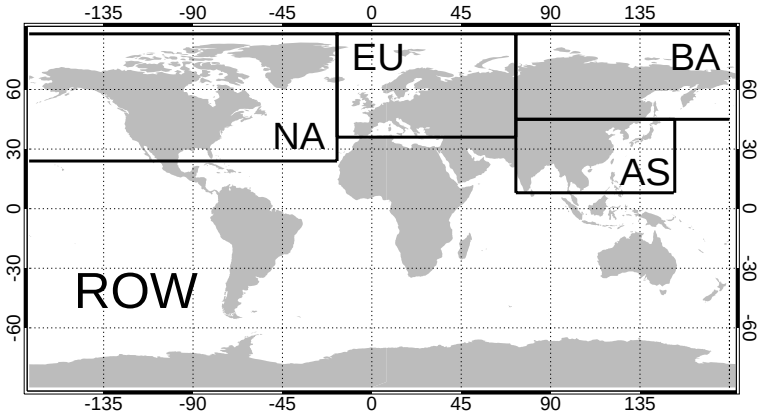

Fig. 3. Source regions for the tagged CO_2 simulation. The regions are denoted boreal Asia (BA), mainland Asia (AS), Europe (EU), North America (NA) and the rest of the world (ROW). See Table 1 for latitude and longitude region definitions and associated flux estimates.

ACPD
8, 7339–7371, 2008

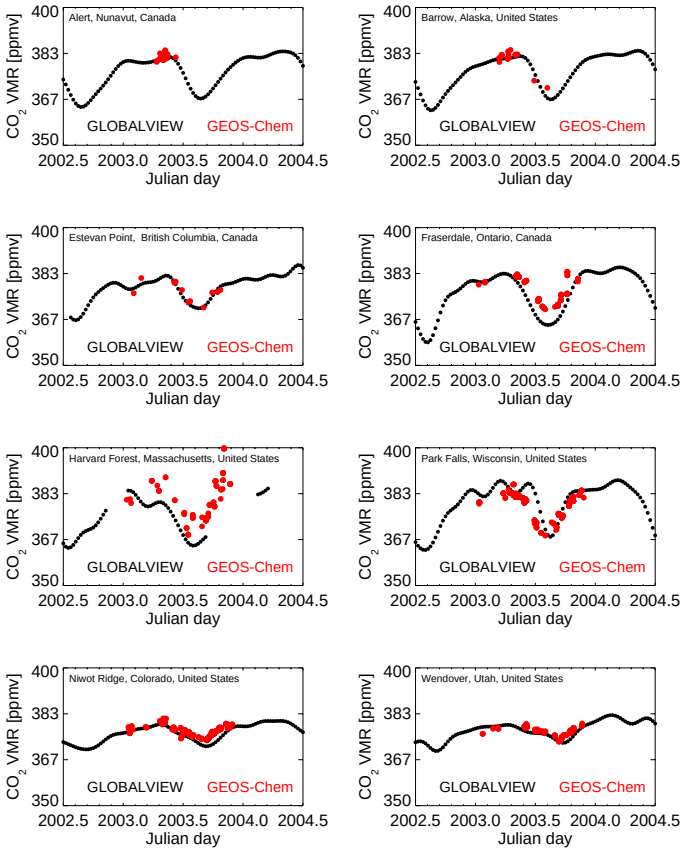

Fig. 4. Comparison of observed (GLOBALVIEW-CO_2, 2006) and model surface CO_2 concentrations (ppmv) over North America during 2003. Model concentrations, averaged on a 2°×2.5°, have been sampled at the overpass time of SCIAMACHY when data are available.

ACPD
8, 7339–7371, 2008

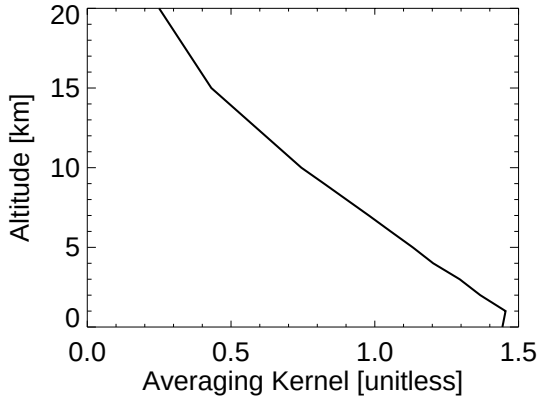

Fig. 5. The mean averaging kernel (0–70° solar zenith angle, SZA) for the retrieval of CO_2 from SCIAMACHY NIR measurements (Barkley et al., 2006c) and applied to the GEOS-Chem model. Individual averaging kernels, representative of a particular SZA, have been generated brute-force by perturbing the US standard atmosphere by 10 ppmv at 1 km intervals between 10 km and at 5 km intervals above 10 km.

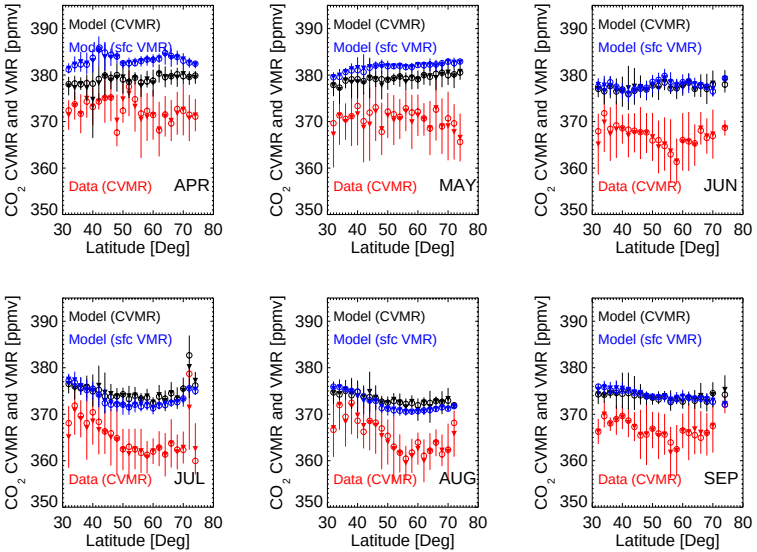

Fig. 6. Monthly mean latitude gradients of SCIAMACHY and GEOS-Chem CO_2 CVMRs (ppmv) and GEOS-Chem surface VMR (ppmv) over North America during April–September 2003 binned every 5° latitude. Model concentrations, averaged on a 2°×2.5°, have been sampled at the overpass time of SCIAMACHY when data are available. Filled triangles denote mean values and open circles denote median values. Vertical lines denote the 1-standard deviation about the mean values.

ACPD
8, 7339–7371, 2008

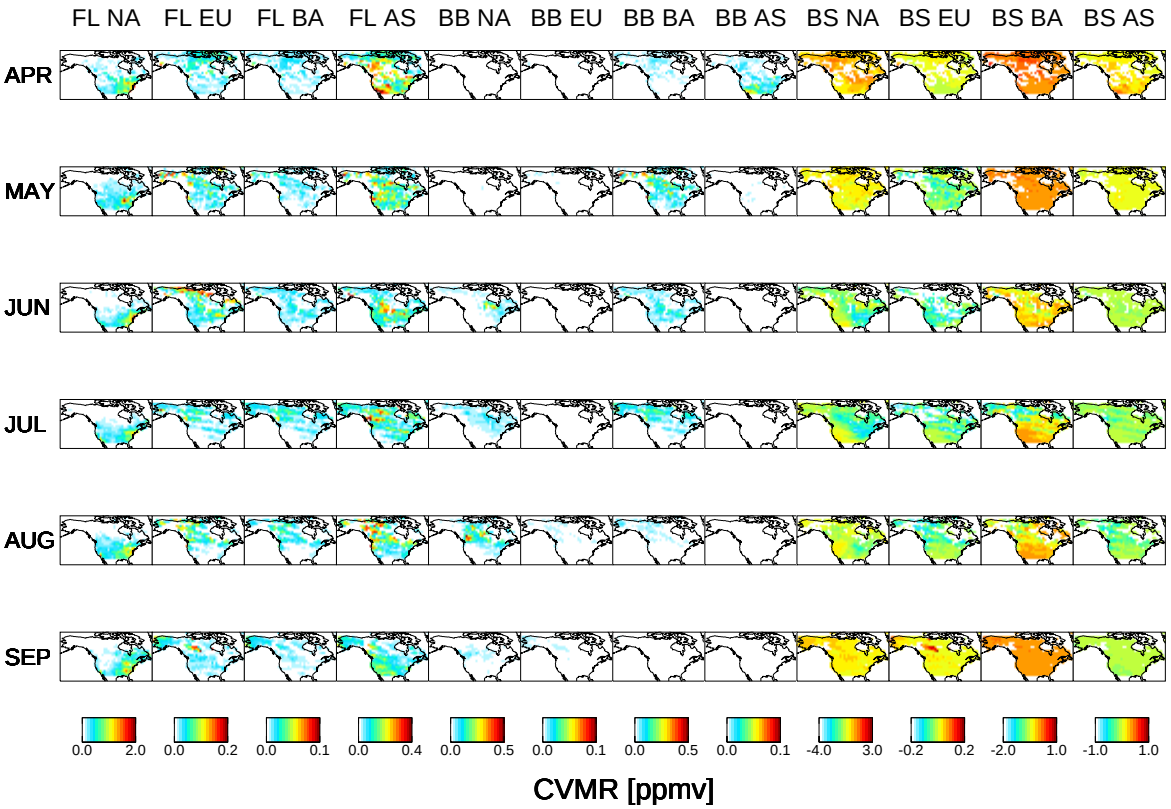

Fig. 7. Monthly mean GEOS-Chem CO_2 CVMR contributions (ppmv) from continental sources and sinks during April to September 2003, averaged over the GEOS-Chem 2°×2.5° grid. See Fig. 3 for source region definitions and Table 1 for regional CO_2 flux estimates.

ACPD
8, 7339–7371, 2008

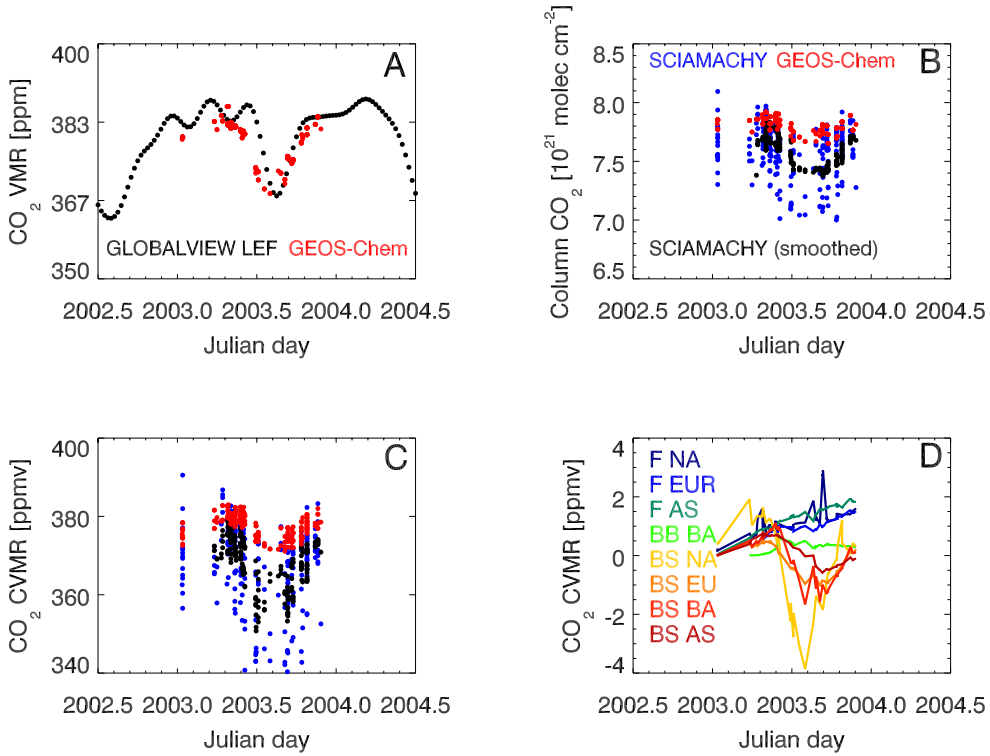

Fig. 8. CO_2 surface concentrations, columns, and CVMRs at the WLEF television tower, Wisconsin USA (45.94° N, 90.27° W, 442 m above sea level) during 2003. **(A)** GLOBALVIEW and GEOS-Chem model, averaged on a 2°×2.5° grid, surface CO_2 concentrations (ppmv), **(B)** SCIAMACHY (raw and 30-point running average) and GEOS-Chem CO_2 columns [10^{21} molec cm^{-2}], **(C)** SCIAMACHY (raw and 30-point running average) and GEOS-Chem CVMR (ppmv), and **(D)** GEOS-Chem CVMR contributions greater than 0.5 ppmv.

ACPD
8, 7339–7371, 2008

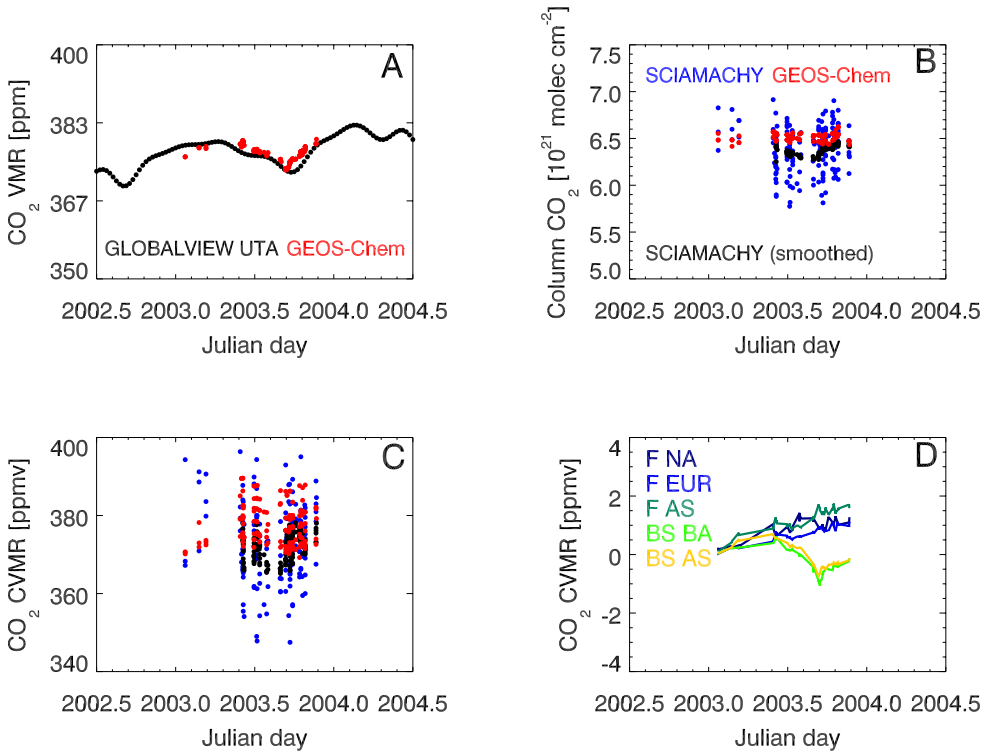

Fig. 9. CO_2 surface concentrations, columns, and CVMRs at Wendover, Utah USA (39.9° N, −113.72° W, 1320 m above sea level) during 2003. Individual panels follow Fig. 8.

ACPD
8, 7339–7371, 2008

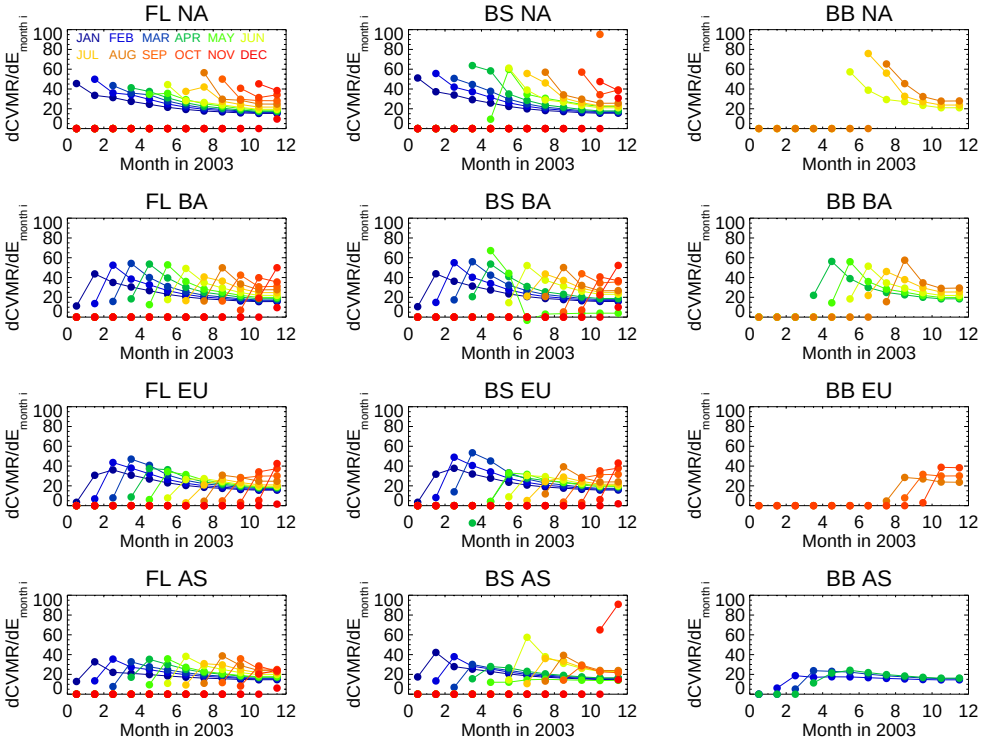

Fig. 10. Monthly mean columns of the Jacobian matrix (ppmv/Tg CO_2), scaled by 10^5 for presentation, calculated using a priori flux estimates (Table 1) and the corresponding GEOS-Chem CVMR contributions, averaged on a 2°×2.5° grid over North America during 2003 (Fig. 7). Colours denote specific months . Each point represents the monthly mean sensitivity of North American CO_2 columns to specific continental sources and sinks. Lines connecting the points have no physical significance.

ACPD
8, 7339–7371, 2008